Faraday Discussions

Accepted Manuscript

This manuscript will be presented and discussed at a forthcoming Faraday Discussion meeting. All delegates can contribute to the discussion which will be included in the final volume.

Register now to attend! Full details of all upcoming meetings: http://rsc.li/fd-upcoming-meetings

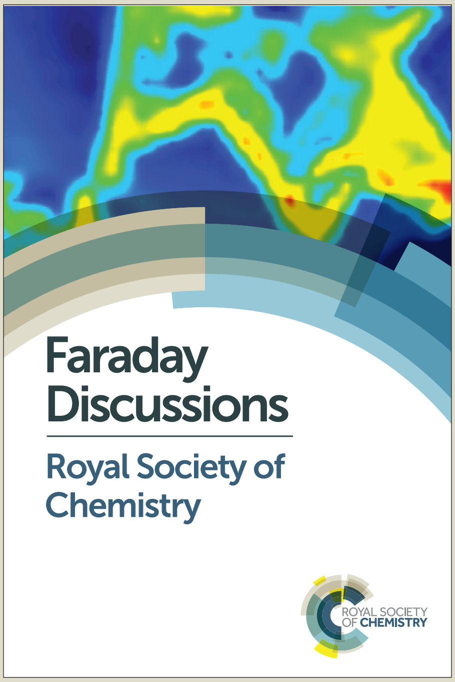

Faraday Discussions

Royal Society of Chemistry

ROYAL SOCIETY OF CHEMISTRY

This is an *Accepted Manuscript*, which has been through the Royal Society of Chemistry peer review process and has been accepted for publication.

Accepted Manuscripts are published online shortly after acceptance, before technical editing, formatting and proof reading. Using this free service, authors can make their results available to the community, in citable form, before we publish the edited article. We will replace this *Accepted Manuscript* with the edited and formatted *Advance Article* as soon as it is available.

You can find more information about *Accepted Manuscripts* in the Information for Authors.

Please note that technical editing may introduce minor changes to the text and/or graphics, which may alter content. The journal's standard Terms & Conditions and the Ethical guidelines still apply. In no event shall the Royal Society of Chemistry be held responsible for any errors or omissions in this *Accepted Manuscript* or any consequences arising from the use of any information it contains.

ROYAL SOCIETY OF CHEMISTRY

www.rsc.org/faraday_d

Introductory Lecture on Corrosion Chemistry: A Focus on Anodic Hydrogen Evolution on Al and Mg

G. S. Frankel, S. Fajardo, and B. M. Lynch
Fontana Corrosion Center, The Ohio State University
Columbus, OH 43210 USA

Abstract

The increase in the rate of hydrogen evolution (HE) on dissolving Mg surfaces with increasing anodic current density or potential, which is sometimes called the negative difference effect, has been the topic of much discussion in recent years. A review of the very recent contributions to this subject is given in this paper. Increased catalytic activity of the corrosion product layer, either from the accumulated impurities or from the Mg oxy-hydroxide itself, is shown to have a minor influence on the anodic HE observed on dissolving Mg at high anodic current densities and potentials. Al exhibits similar characteristics during anodic polarization in concentrated HCl, although the anodic HE rate on Al is less than on Mg. Possible mechanisms for the anodic hydrogen are provided and implications in the area of intergranular corrosion and environmental cracking are discussed.

Introduction

Corrosion, the environmental degradation of materials, involves many aspects of chemistry, as can be seen by the breadth of topics in this meeting and published volume. Details of the environment include: the concentrations of species that might be aggressive, oxidizing, passivating, inhibiting, complexing, or buffering; the temperature, pressure, and flow conditions; the electrochemical potential and distribution across the surface caused by local reactions and ohmic potential drops; atmospheric corrosion parameters such as relative humidity, pollutants, and particulates; and stress conditions such as load and load fluctuations. Details of the material include crystallinity vs. amorphicity, alloy composition, microstructure such as grain size and shape, second phases, inclusions, impurities, precipitates, solute depleted zones, dislocation density and surface films that are protective such as passive films or less protective deposited films. Physical descriptions of the component or test sample of relevance might include size from a massive beam to a nanoparticle, surface preparation, surface roughness, stress-concentrating defects, and physical connections that might cause galvanic coupling or crevices. Corrosion protective schemes are relevant such as a wide variety of possible coatings and potential alteration by cathodic or anodic protection. Considerable focus has been placed on the use and development of advanced techniques for the study of corrosion, including electrochemical approaches, surface analytical methods, scanning techniques that provide spatial resolution, and powerful methods for in situ analysis. Finally, modeling of corrosion processes is an active field that can provide insights and predict behavior with less need for lengthy experiments. A long-term goal of this effort would be to connect the behavior at multiple length scales from atomistic to macroscopic levels in a way that would allow the prediction of component lifetime based on fundamental principles. Many of these topics can be found in the papers and discussions of this meeting and volume.

The purpose of the introductory lecture and paper in a Faraday Discussion meeting and volume, respectively, is to “set the stage.” Owing to the vastness of the field, a comprehensive review is inappropriate and borders on impossible given the page constraints. It was therefore decided to limit the scope to a few issues in the area of localized corrosion and to raise some points that would initiate discussion.

Localized corrosion is a part of the corrosion field that is rich in chemical complexity.[1] Essentially all of the topics listed above can play a role or even be dominant. Pits, crevices and cracks often contain concentrated solution and steep concentration gradients, as well as potential gradients and strong sensitivity to the local potential. Microstructural features often control the severity and nature of the attack.

The introductory lecture covered four aspects of localized corrosion chemistry; this introductory paper will focus on only one of them, the accelerated production of hydrogen gas on dissolving metal surfaces, or anodic hydrogen. The topics that were presented but are not covered in this paper include the mechanism for trenching attack around cathodic particles in Al alloys (pH gradient, potential gradient or interface defects), the electrochemical properties of solute elements in a metal matrix as they combine in the initial stages of particle formation, and the effects of limited water in localized corrosion sites caused by the complexation of ions in the concentrated localized environment.

Hydrogen evolution in Al pits

Anyone who has looked closely at pits in Al has noticed that H_2 bubbles are emitted from actively growing pits and that the hydrogen evolution stops when the pits stop growing. A poster at this meeting displayed this exact phenomenon using high resolution x-ray tomography.[2] The rate of hydrogen evolution (HE) in pits can be quantified under special conditions.

HE from pits in 99.999% Al and two less pure Al alloys polarized in deaerated NaCl solution was studied by Drazic and Popic.[3] They used a rotating ring disk electrode (RRDE) in which the H_2 evolved from pits in the Al disk was oxidized on the Pt ring. Figure 1 shows some of the results of their work. The open symbols represent the measured polarization curve on the disk and the filled symbols show the ring oxidation current. The H_2 oxidation rates on the ring matched the measured currents in the cathodic region of the curve below the corrosion potential. Al is spontaneously passive in this deaerated solution, and the HE rate continued to decrease as the potential increased in the passive region. However, as soon as the current increased as the result of pit initiation, a similarly sharp increase in the rate of HE was detected. The measured HE rate was about 5% of the measured current density. The authors showed similar behavior for the other Al alloys; pitting was always accompanied by a high rate of HE.

Pitting of thin film samples offers another approach for the quantification of HE during pitting. The kinetics of pits in thin film Al samples were first reported 25 years ago.[4] Sputtered Al films, about 100 nm thick deposited onto glass substrates, were tested in chloride solution. Pits in such samples very quickly penetrate the thickness of the metallic coating and reach the inert substrate. This barrier prevents further deepening, and the pits continue to grow by expanding outwards across the substrate with essentially vertical pit walls. The undermined passive film is lifted into the solution during growth by the hydrogen bubbles (more on that later) and

Figure 2a is an SEM image of a pit edge showing the undermined passive film collapsed back onto the surface. The pit growth is two-dimensional (2-D) and the pit takes the form of circles at high applied potentials. At lower potentials the pit perimeter is more convoluted owing to the partial repassivation of the growing pit front. The difference in reflectivity of the Al film and glass substrate allows for the capture of a high contrast image using incident light and a video recording device, Figure 2b.

The original paper described how the anodic pit current density, i_{anod}, could be assessed from the increases in pit perimeter and area with time.[4] A simpler approach is to use the local velocity of the pit radius, v = dr/dt, which is constant for the thin film pits owing to their fixed pit depth:

$$i_{anod} = v\,\frac{\rho n F}{M} \qquad (1)$$

where ρ is metal density, n=3 is the charge on the dissolved Al ion, F is the Faraday constant, and M is the molecular weight. Because v is constant, i_{anod} tends to be constant with time. Values of anodic pit current density as a function of the fixed applied potential are shown as the square symbols in Figure 2c. The anodic current densities are high, on the order of tens of A/cm^2 for pits in films of this thickness. This high current density reflects the very high current density of pits in bulk samples when they are small, on the order of 100 nm in depth.

Evident in Figure 2b is a stream of H_2 bubbles emanating from the growing pit. The current density associated with the HE at thin film pits can be assessed in cases where a single pit forms. In that case, the current measured by the potentiostat is associated only with the one pit. The active pit area can be determined from the film thickness and the perimeter change with time. The measured current, I(t), and the area, A(t), tend to have the same dependence on time so the net current density, $i_{net} = I(t)/A(t)$, is constant with time, like i_{anod}. The HE current density for these pits can then be assessed from:

$$|i_{HE}| = i_{anod} - i_{net} \tag{2}$$

The triangular symbols in Figure 2c represent i_{net} measured for experiments with single pits. As indicated by Equation 2, the HE current density can be assessed by the difference between the i_{anod} and i_{net}. The analysis shows that i_{HE} is huge, on the order of A/cm^2. Figure 1 shows that the rate of HE on Al even at very low potentials in the cathodic region is still 4 orders of magnitude smaller than the rate in these actively growing thin film pits at a much higher potential. Clearly HE can occur in pits at extremely high rates even though Al is not known as a good catalyst for HE. It is of interest to understand how this is possible, and what implications this high rate of HE might have for corrosion and cracking of Al alloys. Before addressing this, the kinetics of HE on Mg and Al will be discussed.

Anodic HE on Mg

In recent years there has been a flurry of activity on a topic related to the high rate of HE in Al pits, enhanced HE on Mg during anodic dissolution, which has been called the negative difference effect (NDE). NDE is an odd term for this phenomenon that is in common use for historical reasons. It will be referred to as "anodic HE" in this paper.

In Figure 3, the rate of HE, assessed volumetrically by hydrogen collection in a burette, is plotted as a function of applied current density during galvanostatic experiments on high purity (HP, 99.98% Mg) and ultra high purity (UHP, 99.9999% Mg) magnesium in 0.1 M NaCl.[5] As the applied negative current decreases, the measured rate of HE decreases, as expected. Although not shown, the measured potential increases as the applied negative current density decreases and then further increases as the applied anodic current density increases above the Mg open circuit potential (OCP). However, as the applied positive or anodic current density increases, the measured rate of HE increases exponentially, in contrast to the continued decrease that is expected with increasing potential for a reduction reaction such as HE. This increase in HE with increasing potential is the phenomenon of anodic HE on Mg. It should be noted that the curves in Figure 3 look like measured polarization curves showing net cathodic and net anodic regions, but all of the data points in the figure represent HE.

Table 1 summarizes many of the explanations for anodic HE in Mg and Mg alloys that have been suggested. A recent review paper presented a current opinion regarding the possible mechanisms of this anodic HE.[6] An overview of some of these mechanisms will be given below along with a summary of new papers published since that recent review paper was written. Indeed, this area is at the moment one of the most rapidly changing topics in the field of corrosion, with new insights being published frequently.

For many years, the most widely discussed mechanism to explain the phenomenon of anodic HE on Mg was univalent Mg, in which some fraction of Mg dissolves into solution as Mg^+, which is then further oxidized chemically with the reduction of water to H_2.[7, 8] According to this theory, higher rates of Mg dissolution would result in more Mg^+ and thus more HE. This theory is consistent with much of the data and can explain apparent observations of $n<2$ at the OCP, where n is the nominal oxidation state of the dissolved ion. A complete critique of this theory will not be attempted here; only a few relevant comments will be offered. There is still no direct evidence for the existence of Mg^+ in solution, as what had been considered the best evidence[9] has been shown to have been the result of other phenomena.[10] Furthermore, the univalent Mg theory is not consistent with apparent observations of $n<1$, for which a theory involving isolated crevice corrosion under H_2 bubbles has been evoked.[11] If this latter mechanism is operative, it would obviate the need for the univalent Mg mechanism, as it alone could explain all observations for $n<2$. In fact, however, the formation of surface films makes the determination of n difficult, so all of the reports of $n<2$ should be viewed with some skepticism. Careful assessments of n by multiple methods have found that indeed $n=2$ for Mg dissolution,[12-14] so the univalent Mg and crevice corrosion mechanisms for anodic HE must also be considered unlikely until clear and direct evidence for their existence is developed.

An alternate explanation for the anodic HE was provided by Frankel et al.[15] Activation-controlled kinetics for the HE reaction (HER) can be described by the Tafel equation as the potentials at which anodic HE on Mg are observed are far below the reversible potential for the HER so the back reaction can be ignored:

$$i_{HER} = i_{0,HER\,on\,Mg} 10^{\left(\frac{-(E-E_{rev,HER})}{b}\right)} \quad (3)$$

where i_{HER} is the HER current density, $i_{0,\text{HER on Mg}}$ is the exchange current density for the HER on Mg, E is the potential, $E_{\text{rev, HER}}$ is the pH-dependent reversible potential for the HER, and b is the Tafel slope. This equation predicts a decrease in the rate of HE as E increases. As shown in Figure 3, this is observed in the cathodic region of Mg polarization, but not in the anodic region. The concept promoted by Frankel et al. was that the catalytic activity of the dissolving Mg surface, as embodied by i_0, increases as the rate of dissolution increases such that the increasing pre-exponential term in Equation 3 dominates the decreasing exponential term.[15] Possible reasons for increased catalytic activity were discussed but no definitive proof was given. Note that this phenomenon might be related to the high rate of HE in pits in Al, which was described above.

Recent papers have focused attention on the role of corrosion films and impurity enrichment in providing the increased catalytic activity of the dissolving surface. When Mg corrodes at the OCP and during anodic polarization, a dark corrosion film forms and this film has some special properties. A related phenomenon is the enrichment of impurity or alloying elements in or under the corrosion film. These topics will be discussed presently with a focus on recent reports.

A study by Williams et al. used the scanning vibrating electrode technique (SVET) to map the net current flowing from a Mg surface during anodic polarization in 2 M NaCl solution.[16] The attack progressed as dark filiform tracks or expanding rings across the surface, depending on the purity, and the active anode sites could be easily distinguished by SVET, Figure 4a. Interestingly, the SVET could also sense regions where the net current was negative, even during anodic galvanostatic polarization at +1 mA/cm^2. The cathodes were the dark oxide left in the wake of the moving anodes. The integrated anodic and cathodic currents both increased with time, but summed more or less to the applied current, which was constant. The integrated cathodic current during anodic polarization increased with increasing applied current density and was found to be slightly less than the volume of hydrogen gas collected using a burette. The observation of net cathodes on an anodically polarized surface is stunning and provides evidence for the importance of the remnant corrosion layer in the anodic HE reaction. The schematic provided in Figure 4b shows how a fraction of the anodic current can be consumed by HE occurring at the neighboring sites covered with corrosion product.[16] The area covered by the dark corrosion product increased with time in the initial stages similarly to the increase in cathodic current measured by the SVET. However, at steady state the rate of HE measured volumetrically is normally constant with time, rather than increasing with time, and it varies with the anodic current density. This constant and current-dependent rate of HE is not consistent with the dark areas being the location of the anodic HE. Furthermore, at steady state, the integrated cathodic current from the SVET is much less than the volumetric HE rate,[17] which indicates that the dark corrosion product regions, which are net cathodes cannot be the source of most of the anodic HE under those conditions.

The robustness of the cathodic activity of the corroded surface was shown by Birbilis et al. using experiments in 0.1 M NaCl on pure Mg that was alternately polarized galvanostatically in the anodic direction and then potentiostatically at -1.9 V SCE, which is cathodic polarization.[18] The current measured during the cathodic polarization step increased as the prior applied anodic current density increased, Figure 5. These findings support those of Williams et al.[16] regarding the catalytic nature of the corrosion product film. However, the measurements of enhanced cathodic reaction were made in the cathodic region, and the relevance to anodic polarization conditions must be confirmed.

The enhanced catalytic activity described above might be associated with the magnesium oxy-hydroxide corrosion film or with impurities enriched either within or under the film. Even the purest Mg available will have impurities that might enrich on the surface during anodic polarization owing to incongruent dissolution of Mg at potentials that are far below the reversible potentials for the impurity metal dissolution. These surface-enriched impurity elements, such as Fe, would be polarized during Mg dissolution at potentials at which they would be expected to exhibit high rates of HE. As a result, a small enrichment of these elements on the surface, in the oxide, or under the oxide, might be the cause of the anodic HE during Mg dissolution. However, the thick corrosion product complicates the measurement of this enrichment.

Analytical transmission electron microscopy measurements on a cross section of a polarized pure Mg surface were performed by Tahiri et al.[19] The corrosion product was found to be bilayered with a crystalline oxide inner layer and a crystalline columnar oxy-hydroxide outer layer. Very small Fe-rich particles, on the order of hundreds of nm in size, were found in the outer layer, as shown in Figure 6. Such sites might be the source of the enhanced catalytic activity of the corrosion film described by Williams et al.[16] However, to do so, some of the electrons generated at the dissolving anode sites would have to conduct through the thick oxide layer to the Fe-rich particles embedded in the outer portion of the oxide, and MgO is not expected to be a good electronic conductor.

Another possibility is that the primary location of impurity element enrichment is beneath the oxide corrosion product layer. Cain et al. used Rutherford Backscattering Spectrometry (RBS) on pure Mg samples following anodic polarization and chromic acid cleaning to remove the oxide product layer.[12] RBS is ideally suited for the sensing of heavy metals concentrated on the surface of lighter metals. Figure 7 shows the results of an analysis of the RBS data, which indicates an increase in the Fe/Mg ratio near the surface (under the removed oxide product layer). The authors suggest that the enrichment efficiency is low owing to possible incorporation of the Fe into a non-conducting oxide layer or release (presumably non-Faradaic) of Fe-rich particles into the solution. However, if such release occurred, the particles would reach their own open circuit potential independent of that of Mg, dissolve into solution, and replate back onto conductive surface sites as elemental Fe. The constant rate of HE with time on an anodically polarized Mg surface is not consistent with the expected continual enrichment of impurity or alloying elements over time. A low enrichment efficiency with no replating resulting in a steady-state surface concentration would be necessary for these surface enriched elements to be the site of anodic HE.

The cathodic behavior of prepolarized Mg samples with 40 or 200 ppm Fe was compared to that of Mg-Fe alloys with a range of Fe content to assess the extent and effect of surface enrichment.[20] The cathodic current at -1.9 V SCE in 0.1 M NaCl after prior anodic polarization was compared to the value expected if all of the Fe were retained on the surface as a result of the anodic prepolarization by comparison with the currents measured on the different alloys without prior anodic polarization. A factor termed the Fe enrichment efficiency was found to be quite low, less than 1%. The factors mentioned above, incorporation into the oxide or non-Faradaic release, were offered as explanations. The authors suggest that "the enhanced HER on anodically polarised Mg is not completely dictated by the Fe concentration in the Mg matrix" and that surface enriched Fe might not be the cause of anodic HE.[20] As intuitive as it seems, the enrichment of Fe and other impurity elements apparently play a minor role in anodic HE. The similarity in anodic HE rate for Mg binary alloys with high concentrations of Fe, Li or Ca to that of pure Mg[21] and ultra high purity Mg (99.9999% pure)[5] supports this finding.

The other aspect of the corrosion product that might be important in the anodic HE process is the Mg oxy-hydroxide layer itself. The notion that such a layer is catalytic toward the HER is, in contrast, non-intuitive. However, another report has found evidence for this type of behavior. Salleh et al. investigated the cathodic behavior of pure Fe and pure Mg electrodes that were hydroxide coated by immersion in a super-saturated $Mg(OH)_2$ solution.[22] The HER kinetics on uncoated and $Mg(OH)_2$-coated Fe were high and essentially the same, suggesting that the hydroxide coating does not block the HER on Fe, Figure 8. The kinetics on Mg and $Mg(OH)_2$-coated Mg were much lower, but the kinetics on the hydroxide coated Mg electrode were about 10x higher than on the uncoated Mg. This remarkable finding takes the focus away from the impurity enrichment and places it on the Mg corrosion product. However, like the influence of impurity enrichment, this notion is not consistent with the observation of a constant HE rate with time for samples in which the corrosion sites move across the surface, resulting in an increasing surface coverage of the corrosion product.

The pH dependence of anodic HE on Mg was investigated using two different methods.[23] Volumetric collection of hydrogen was performed in chloride-free buffer solutions of pH 3, 7, and 10. The hydrogen volume increased with decreasing pH owing to the increase in the corrosion rate. Anodic HE was observed at all pH values, but the relative amount was larger at the higher pH. In pH 3 and 7 buffers, the HE rate decreased with increasing applied current just above the OCP, and anodic HE was only observed at higher anodic current densities. Also, yet higher current densities were required to observe anodic HE when the buffer strength was larger. This suggests that pH changes are important for anodic HE such that it only occurred when the buffering capacity was locally overwhelmed. Measurements were also performed in a flow cell connected to an inductively coupled plasma – mass spectrometry (ICP-MS) unit. Anodic HE was also not observed in the flow cell at low current densities, as the flowing condition prevented anodic HE at current densities for which it was observed in volumetric measurements. The pH changes seem to be related to the stability of surface films, indicating the importance of such films in the anodic HE process.

A study by the authors of this work provides evidence that neither surface-enriched impurity elements nor the Mg oxy-hydroxide corrosion product dominate the anodic HE phenomenon.[5] As shown in Figure 3, high purity (HP, 99.98%) and ultra high purity (UHP, 99.9999% Mg) were tested by volumetric collection of hydrogen during galvanostatic polarization. The rate of anodic HE was only slightly higher on HP than on UHP Mg; extremely high rates of anodic HE were still observed on the UHP Mg, which has only 1 ppm total impurity, in line with the apparent minor effect of impurity elements on anodic HE. Following anodic polarization, cathodic polarization curves were measured in fresh 0.1 M NaCl solution, Figure 9. As found previously,[18] the cathodic current densities were higher after the anodic prepolarization, and generally increased with increasing anodic current density, even though the total charge was constant. Also, the currents on the HP Mg were higher than on the UHP Mg for the same pretreatment. These observations provide more support for the notion of some cathodic enhancement by the corrosion film and/or enriched impurities, even though the UHP Mg had very low impurity content.

The previous paper then analyzed the data in Figure 9 to show that this enhancement in the rate of the cathodic reaction plays a small role in anodic HE phenomenon. The primary assumptions were that the corrosion film and accumulated impurities formed during anodic polarization are robust, so that the surface during cathodic polarization reflects the condition during the prior anodic polarization, and that the enhancement in the cathodic reaction is the same mechanism that operates at anodic potentials. It is therefore possible to assess the anodic HE rate associated with the corrosion film and impurities by extrapolation of the behavior in the cathodic region to the potentials reached during the prior anodic polarization. The procedure used for the extrapolation is clarified in Figure 10. This figure reproduces a few of the cathodic polarization curves for UHP Mg from Figure 9 and overlays the current density calculated from the volumetric HE measurements during galvanostatic polarization plotted against the IR-corrected measured potential during those measurements. The cathodic polarization curves are not IR-corrected, so there is no clear Tafel region and extrapolation is difficult. These curves were each extrapolated by using the Tafel slope determined from the cathodic volumetric measurements at the tangent point to the curves. The lines in Figure 10 show the extrapolation for the case of polarization of UHP Mg at 1 mA/cm^2. The arrow pointing to the right at about 2 x 10^{-5} A/cm^2 is the value predicted for the HE rate from the film and impurities at the IR-corrected potential measured during the galvanostatic polarization, about -1.69 V SCE. This value is much lower than the rate of HE measured volumetrically, which was equivalent to about 4 x 10^{-4} A/cm^2. Other approaches to extrapolation are possible, but it is clear from this figure that the values would in any case be much lower than the measured rates of HE in the anodic region.

Figure 11 shows the predicted values of anodic HE rate from the corrosion film and accumulated impurity elements determined by the extrapolation of the cathodic polarization curves. The rates are almost independent of the applied anodic current density and are about 10x larger for HP Mg than for UHP Mg. So the impurity level of the Mg plays a role in the anodic HE process, but this role is small. The anodic HE rates for the pretreated UHP Mg are close to that for untreated UHP Mg at the OCP. The value for 0.5 mA/cm^2 is anomalous and a discussion of this point can be found in the original paper.[5]

As noted above, the rate of HE might increase on a dissolving surface because of an increase in the catalytic activity of the dissolving area. It can be assumed that the total rate of anodic HE is the sum of the HER occurring on the previously corroded surface, which itself is the sum of the HE on the corrosion film and that associated with accumulated impurities, and the HER occurring at the actively dissolving anode sites:

$$HE_{total} = HE_{anode} + HE_{film} + HE_{impurities} \qquad (4)$$

A schematic for this process is shown in Figure 12. It differs from the mechanism in Figure 4 by noting the HE occurring on the film and impurities separately, and including HE_{anode}. The corrosion attack is shown in this figure as progressing from left to right, leaving behind a corroded area. Knowing the total rate of anodic HE from volumetric measurements and using the rate of anodic HE associated with the film and impurities, $HE_{film} + HE_{impurities}$, determined by the extrapolation method described above, it is possible to assess the anodic HE rate associated with the actively dissolving anodic regions, HE_{anode}. Figure 13 shows the different components of the anodic HE. The dashed lines represent HE_{total} measured volumetrically. The symbols represent HE_{anode}, which were determined by subtracting the values of $HE_{film} + HE_{impurities}$ at each applied current density given in

Figure 11 from HE_{total}. It is clear that anodic HE rates from the film and impurities are small and that HE_{anode} is close to HE_{total}, especially for the higher applied current densities.

A mechanism focused on the actively dissolving anodic regions as the primary site for anodic HE is not inconsistent with the observations described above. Enhanced HER during cathodic polarization for a sample that was previously polarized anodically is strong evidence for the effects of the corrosion film and surface-enriched impurities. These factors might play a significant role during cathodic polarization and OCP dissolution, but their effects appear to be small under the conditions of anodic polarization. The SVET observations of distinct cathodic regions are also not inconsistent because the SVET only measures net current from spatially separated regions and so is not sensitive to a cathodic reaction co-located with a larger anodic reaction, which would be sensed as a net anodic region.

Anodic HE on Al

It was shown above that HE occurs in actively growing pits in Al at high rates. Owing to gradients in potential and chemistry as well as changing active area, factors that are inherent in all pits, it is not possible to assess the kinetics of HE in a controlled fashion as has been done for Mg as long as the corrosion morphology includes pitting. As a result, work was undertaken to find conditions of nominally uniform corrosion of Al and then measure the anodic HE.

According to the Pourbaix diagram, Al forms a protective layer of Al oxide (Al_2O_3) in neutral solutions. This oxide is amphoteric, dissolving to form aluminate and Al^{3+} ions at high and low pH, respectively. This prediction, which is based on thermodynamics, would indicate that pitting corrosion should occur only in neutral solutions because a stable passive film is required for the establishment of pitting. The first approach taken to address anodic HE in Al was to study the behavior in alkaline solutions, which are commonly used for etching of Al. Anodic HE was not observed in very alkaline solutions; the HE rate decreased with increasing applied anodic current density as expected from the Tafel Law, Equation 3.

Passivity should also be absent in low pH solutions. Furthermore, the pH of pit environments in Al has been measured to be 3,[24] so film-free dissolution should be possible in HCl solutions of this pH and lower. However, some retained passivity and pit formation can be observed on surfaces of pure Al samples polarized to high potentials in HCl solutions with concentrations as high as 4 M. Figure 14 shows polarization curves for 99.99% Al in 1 M and 12.1 M HCl. The polarization curve in 1 M HCl shows a clear passive region and breakdown potential. The surface following polarization exhibits a high density of crystallographic pits but also clear evidence of unattacked passive surface, Figure 15a. This shows stability of passive film to very low pH values and suggests that the pit environment has a pH much lower than 3. Beck reported that the pH drops precipitously as the $AlCl_3$ concentration approaches saturation, reaching as low as -0.25.[25] However, the presence of crystallographic pits rather than polished pits suggests that the pit solution was not saturated, and the copious hydrogen bubble evolution should effectively mix the pit environment with the bulk environment.

The polarization curve measured in 12.1 M HCl, which was taken directly from the acid bottle without dilution, exhibited active dissolution followed by an apparent active/passive transition, Figure 14. The cause of this behavior is unknown, but it was reproducible and the current decrease was accompanied by an observable cessation of HE. The passive behavior was short-lived as the current increased again to very high values within about 100 mV. Following polarization, the surface was roughened, with more attack at grain boundaries, but no evidence of pitting, Figure 15b.

The absence of pitting in 12.1 M HCl allowed the HE rate to be measured during anodic galvanostatic polarization, Figure 16. The HE rate decreased as the applied anodic current density increased to 5 mA/cm^2. However, as the current density was increased further, the rate of HE increased substantially, providing clear evidence for anodic HE in Al, even in the absence of pitting corrosion. The amount of anodic HE was approximately 20% of the net applied current, which is similar to the values determined in the Al thin film pitting experiments mentioned above.[4] However, this amount is less than that found on Mg, which has been found to be about 50% of the net applied anodic current.[15]

As was done for Mg, cathodic potentiodynamic polarization measurements were performed on the Al samples following the anodic galvanostatic polarization. In contrast to Mg, these samples exhibited decreased cathodic reactivity compared to a sample that was not prepolarized, Figure 17, indicating that robust catalytic enhancement of the surface is not required for anodic HE. It should be noted that precipitation of an Al corrosion product film is also not expected for this solution.

Mechanism of Anodic HE

As described above, the increasing rate of HE with increasing applied anodic current density or potential can be explained by an increase in the exchange current density that overcomes the decreasing exponential term containing the potential. The question is of course why this would happen. One approach to providing an explanation is from the definition of the exchange current density that falls out of the development of the Butler Volmer equation. The formalism presented by Bockris and Reddy[26] will be used here. The current density for an activated process can be assessed from the activation energy using the Arrhenius equation:

$$i = \frac{FkT}{h} c_i e^{-\Delta G^{0\neq}/RT} \qquad (5)$$

where F is the Faraday constant, k is the Boltzmann constant, T is temperature, h is the Planck constant, c_i is ionic concentration, $\Delta G^{0\neq}$ is the activation energy and R is the ideal gas constant. The work associated with moving a charged species through a portion of the potential drop across the double layer (the portion to the activated state) is added to the chemical activation energy:

$$\Delta G^{0\neq} = \Delta G^{0\neq}_{chem} + \beta e_0 \Delta\phi \qquad (6)$$

where $\Delta G^{0\neq}_{chem}$ is the chemical component of the activation energy, β is the symmetry factor, e_0 is the elemental charge, and Δϕ is the potential drop across the double layer. Substituting Equation 6 into Equation 5, one arrives at the Tafel equation, Equation 3, with the exchange current density defined as:

$$i_0 = \frac{FkT}{h} c_i e^{-\Delta G^{0\neq}_{chem}/RT} \qquad (7)$$

It is therefore reasonable to consider that the exchange current density is determined primarily by the chemical activation energy of the electron transfer process, $\Delta G^{0\neq}_{chem}$, and that a decrease in this value would lead to an increase in i_0. Again, if this decrease in $\Delta G^{0\neq}_{chem}$ were larger than the increase in $\beta e_0 E$, then the total rate of the cathodic reaction would increase with increasing E.

One approach to addressing $\Delta G^{0\neq}_{chem}$ is through density functional theory (DFT). DFT is a powerful approach for addressing issues in corrosion science, as is described by several papers in this meeting and volume. The approach has been used to probe the likely pathways for the HER on an Mg(0001) surface.[27] Considering elemental steps of the process separately, the activation energies for different transition states were calculated. Those with the lowest activation energy were considered most likely. This approach might be used to address changes in i_0 that might occur during dissolution. For example, it is possible that the dissolving Mg or Al surface is always filmed, even during high rate dissolution. This is not unreasonable given the extreme reactivity of these metals in the unoxidized state. If the chemical activation energy decreases as dissolution increases owing to a change in the nature of the surface such as a surface film, then the rate of the HER would increase with increasing E.

Another explanation for the increase in anodic HE with potential involves an increase in the number of active sites with increasing dissolution rate. For this to explain anodic HE, the rate of increase of the sites must be greater than the decreasing driving force for the reaction caused by the increasing potential. It can be shown that the validity of this explanation will depend on the relative kinetics of the anodic dissolution reaction and the HER.[28]

Possible implications for anodic HE in Al

There are several implications for the high rate of anodic HE in pits and other forms of localized corrosion in Al and Al alloys. One aspect is the moderating effect that the local cathodic reaction would have on the local pH. As mentioned above, high concentrations in the pit solution should be prevented by the strong evolution of hydrogen bubbles, but the co-location of the HER at a sizeable rate will also prevent the development of low pH values at the site of the anodic reaction.

Another role that high rates of HE in pits and cracks might play is related to environmental cracking. Although for Al alloys it is difficult to make a clear distinction between anodic effects on cracking and the role of hydrogen, which is always present during localized corrosion of Al, a strong case has been made for the embrittlement by hydrogen playing a significant role.[29, 30] An interesting example is the situation of AA5083, an Al-Mg alloy that can form β phase, Al_3Mg_2, along grain boundaries during prolonged exposure at intermediate temperatures that can be experienced, for instance, in service in certain maritime applications.[31-33] The β phase is anodic to the matrix and preferentially dissolves. When sufficient grain boundary β phase is present, the alloy is considered to be sensitized and will exhibit intergranular corrosion (IGC) and intergranular stress corrosion cracking (IGSCC) in chloride-containing environments. This explanation for the IGSCC susceptibility of sensitized AA5083 by the anodic dissolution of grain boundary β phase makes perfect sense, except that transmission electron microscopy imaging of even highly sensitized material does not reveal continuous β phase along the grain boundaries.[33] In fact, intergranular fracturing of highly sensitized AA5083 by Ga embrittlement, which does not cause corrosion and thus preserves the details of the grain boundary fracture surface, reveals distinctly discontinuous β phase particles along the grain boundary.[34] The sustained intergranular fracture of the grain boundary ligaments between the β particles has been explained by a hydrogen embrittlement mechanism, such that the total fracture mechanism involves coupled dissolution of the β phase particles and hydrogen embrittlement.[35] HE at the crack tip in association with the localized anodic dissolution creates atomic H, which can be absorbed by the Al, transported to the fracture process zone preceding the crack tip, and result in embrittlement of the β-free grain boundary regions. Acidification caused by aluminum ion hydrolysis was described as being critical in promoting hydrogen evolution.[35] However, the high rate of anodic HE that likely occurs at the crack tip probably allows H to play a role independent of the crack solution acidification by hydrolysis. This possibility of high rate anodic HE influencing SCC has already been suggested.[36]

It is also possible that anodic HE promotes an embrittlement effect even in the absence of an applied stress, resulting in a hydrogen-related mechanism for nominally unstressed IGC in high strength Al alloys. The application of a strain causing a stress of less than 10% of the yield stress along the through thickness direction of a plate of AA2024-T3 resulted in a sizeable increase in the rate of IGC under aggressive conditions, essentially causing IGSCC.[37] Given this low threshold for the acceleration of intergranular attack, it seems that the corrosion product could provide enough stress to drive the attack, and that the concomitant anodic HE within the IGC site/crack might play a role in driving the IG separation.

Concluding Remarks

This introductory paper has focused on a particular topic, the increase in the rate of the HER with increasing potential on actively dissolving Mg and Al surfaces, which is sometimes referred to as the negative difference effect. This topic is only a small part of the vast field of corrosion chemistry, but it embodies many of the important aspects of corrosion that were listed in the introduction: strong potential and compositional gradients, transport, metal composition and microstructure, stress effects, advanced analytical methods and modeling. It is also a somewhat controversial issue that has attracted a lot of attention recently, so it is a good topic to set the stage for discussions on corrosion chemistry.

The recent literature in the area of anodic HE on Mg has focused on the role of the corrosion product layer, both accumulated impurity atoms in or below the layer, as well as the nature of the Mg oxy-hydroxide itself. A careful analysis indicates that this product layer and accumulated impurities cannot play a large role in the high levels of HE found during anodic polarization of Mg at high currents or potentials. Eliminating these aspects leaves the site of the anodic reaction as the location for most of the anodic HE. A convenient way to consider this effect is through changes in the exchange current density for the HER, which might be controlled by the chemical activation energy associated with details in the surface characteristics.

Analogous HE on dissolving Al was found in concentrated HCl, an environment in which pitting corrosion does not occur. The rate of anodic HE on Al is less than on Mg, but that is not unexpected as Mg is a more reactive element. The exact mechanism for the increase in the rate of HE with increasing potential on Mg and Al is not clear at this point. However, several testable hypotheses have been suggested, as listed in Table 1, and it is expected that a verified and agreed upon understanding will develop in the coming years.

References

1. G. S. Frankel, *Journal of the Electrochemical Society* **145**, 2186-2198 (1998).
2. S. Glanvill, A. du Plessis, S. Street, M. Basham, T. Rayment and A. Davenport, In situ tomographic investigations of initiation of localised corrosion of aluminium alloy AA2024, poster presentation at Faraday Discussion: Corrosion Chemistry, London, 2015.
3. D. M. Drazic and J. P. Popic, *Journal of Applied Electrochemistry* **29**, 43-50 (1999).
4. G. S. Frankel, *Corrosion Science* **30**, 1203-1218 (1990).
5. S. Fajardo and G. S. Frankel, *Electrochimica Acta* **166**, 255-267 (2015).
6. S. Thomas, N. V. Medhekar, G. S. Frankel and N. Birbilis, *Current Opinion in Solid State & Materials Science* **19**, 85-94 (2015).
7. A. Atrens and W. Dietzel, *Advanced Engineering Materials* **9**, 292-297 (2007).
8. G. Song, A. Atrens, D. Stjohn, J. Nairn and Y. Li, *Corrosion Science* **39**, 855-875 (1997).
9. R. L. Petty, A. W. Davidson and J. Kleinberg, *Journal of the American Chemical Society* **76**, 363-366 (1954).
10. A. Samaniego, B. L. Hurley and G. S. Frankel, *Journal of Electroanalytical Chemistry* **737**, 123-128 (2015).
11. Z. M. Shi, F. Y. Cao, G. L. Song and A. Atrens, *Corrosion Science* **88**, 434-443 (2014).
12. T. Cain, S. B. Madden, N. Birbilis and J. R. Scully, *Journal of the Electrochemical Society* **162**, C228-C237 (2015).
13. L. Rossrucker, K. J. J. Mayrhofer, G. S. Frankel and N. Birbilis, *Journal of the Electrochemical Society* **161**, C115-C119 (2014).
14. J. Swiatowska, P. Volovitch and K. Ogle, *Corrosion Science* **52**, 2372-2378 (2010).
15. G. S. Frankel, A. Samaniego and N. Birbilis, *Corrosion Science* **70**, 104-111 (2013).
16. G. Williams, N. Birbilis and H. N. McMurray, *Electrochemistry Communications* **36**, 1-5 (2013).
17. G. Williams, personal communication, 2015.
18. N. Birbilis, A. D. King, S. Thomas, G. S. Frankel and J. R. Scully, *Electrochimica Acta* **132**, 277-283 (2014).
19. M. Taheri, J. R. Kish, N. Birbilis, M. Danaie, E. A. McNally and J. R. McDermid, *Electrochimica Acta* **116**, 396-403 (2014).
20. D. Lysne, S. Thomas, M. F. Hurley and N. Birbilis, *Journal of the Electrochemical Society* (2015).
21. A. Samaniego, N. Birbilis, X. Xia and G. S. Frankel, *Corrosion* **71**, 224-233 (2015).
22. S. H. Salleh, S. Thomas, J. A. Yuwono, K. Venkatesan and N. Birbilis, *Electrochimica Acta* **161**, 144-152 (2015).
23. L. Rossrucker, A. Samaniego, J.-P. Grote, A. M. Mingers, C. A. Laska, N. Birbilis, G. S. Frankel and K. J. J. Mayrhofer, *Journal of the Electrochemical Society* **162**, C333-C339 (2015).

24. K. P. Wong and R. C. Alkire, *Journal of the Electrochemical Society* **137**, 3010-3015 (1990).
25. T. R. Beck, *Electrochimica Acta* **29**, 485-491 (1984).
26. J. O. M. Bockris, A. K. N. Reddy and M. Gamboa-Aldeco, *Modern Electrochemistry 2A*, Kluwer Academic, New York (2000).
27. K. Williams, personal communication, 2015.
28. R. C. Newman, personal communication, 2015.
29. R. P. Gangloff, in *Enginering Materials Advisory Services*, A. Blom, ed., p. 3401-3433, West Midlands, UK, (2002).
30. J. R. Scully, G. A. Young and S. W. Smith, *Gaseous Hydrogen Embrittlement of Materials in Energy Technologies, Vol 1: The Problem, Its Characterisation and Effects on Particular Alloy Classes*, 707-768 (2012).
31. D. R. Baer, C. F. Windisch, M. H. Engelhard, M. J. Danielson, R. H. Jones and J. S. Vetrano, *Journal of Vacuum Science & Technology a-Vacuum Surfaces and Films* **18**, 131-136 (2000).
32. J. R. Pickens, J. R. Gordon and J. A. S. Green, *Metallurgical Transactions a-Physical Metallurgy and Materials Science* **14**, 925-930 (1983).
33. J. L. Searles, P. I. Gouma and R. G. Buchheit, *Metallurgical and Materials Transactions a-Physical Metallurgy and Materials Science* **32**, 2859-2867 (2001).
34. N. Birbilis, R. Zhang, M. L. C. Lim, R. K. Gupta, C. H. J. Davies, S. P. Lynch, R. G. Kelly and J. R. Scully, *Corrosion* **69**, 396-402 (2013).
35. C. B. Crane, *Validation of the Coupled Dissolution-Hydrogen Embrittlement Mechanism of IGSCC in Low Temperature Sensitized AA5083-H131* PhD Thesis, University of Virginia (2013).
36. D. M. Drazic and J. P. Popic, *The negative difference effect and stress corrosion cracking*, p. 111-120 (1999).
37. X. D. Liu, G. S. Frankel, B. Zoofan and S. I. Rokhlin, *Corrosion Science* **46**, 405-425 (2004).

Table 1. Possible mechanisms for anodic HE

Mechanism	**References**	**Comment**
Univalent Mg	[7, 8]	Has been criticized in recent years
Crevice corrosion under H_2 bubbles	[11]	No evidence
Surface area increases		Cannot explain order of magnitude increases
Tafel slope changes		No strong evidence
Chunking (non-Faradaic loss of Mg metal)		No strong evidence
Deposition of impurities from solution		No strong evidence
pH change	[23]	Plays a role
Surface enrichment of impurities	[12, 20]	Plays a role
Corrosion product coverage and catalytic activity	[16, 18, 19, 22]	Plays a role
Catalytic nature of dissolving surface	[5]	Potentially plays a dominant role

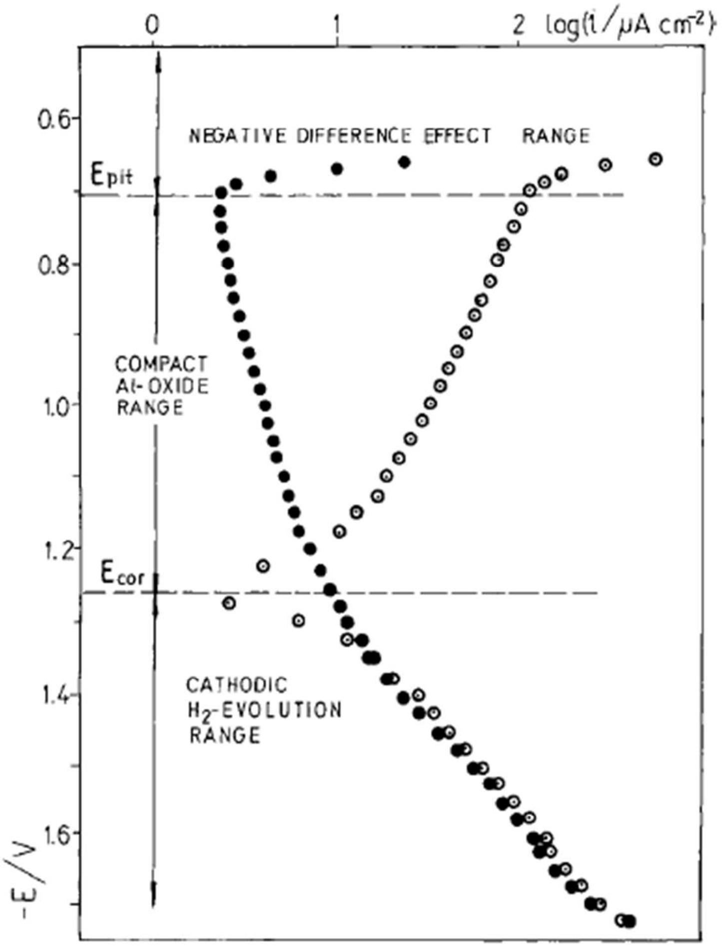

Figure 1. HE rate during the polarization of a rotating Al disk.[3] Open symbols represent the measured current density and the closed symbols are the ring current associated with oxidation of hydrogen at the ring. With kind permission from Springer Science and Business Media.

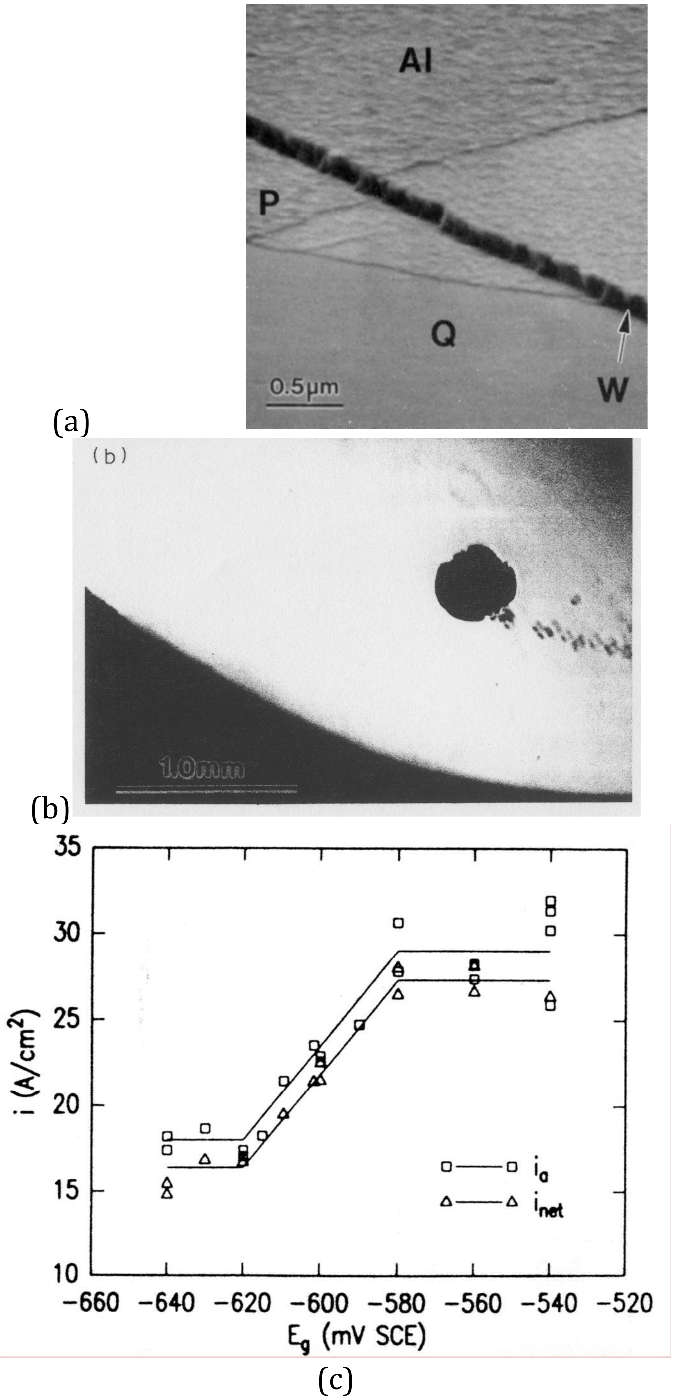

Figure 2. Results of 2-D pit growth experiments.[4] a) SEM image of the sample after 2-D pit growth where Q is the quartz substrate, P is the passive film and W is the 2-D pit wall, b) optical image during a pit growth experiment showing hydrogen bubbles streaming upwards from the pit surface. c) anodic and net current density as a function of applied potential. The lines are added to aid assessment, and the difference between the two is the current density associated with HE. Reprinted with permission from Elsevier.

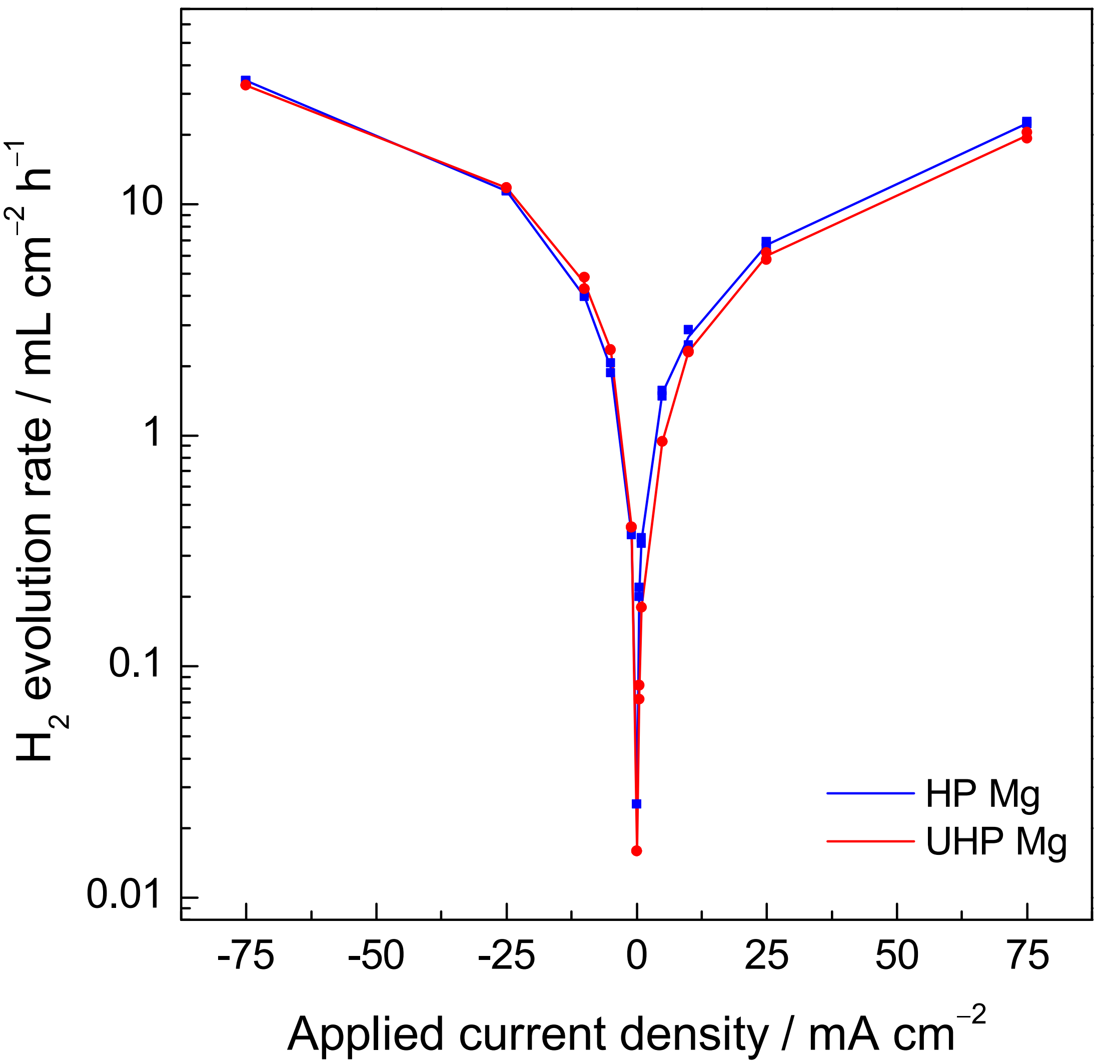

Figure 3. HE rate determined volumetrically for high purity (HP) and ultra high purity (UHP) Mg samples as a function of the applied current density.[5] Reprinted with permission from Elsevier.

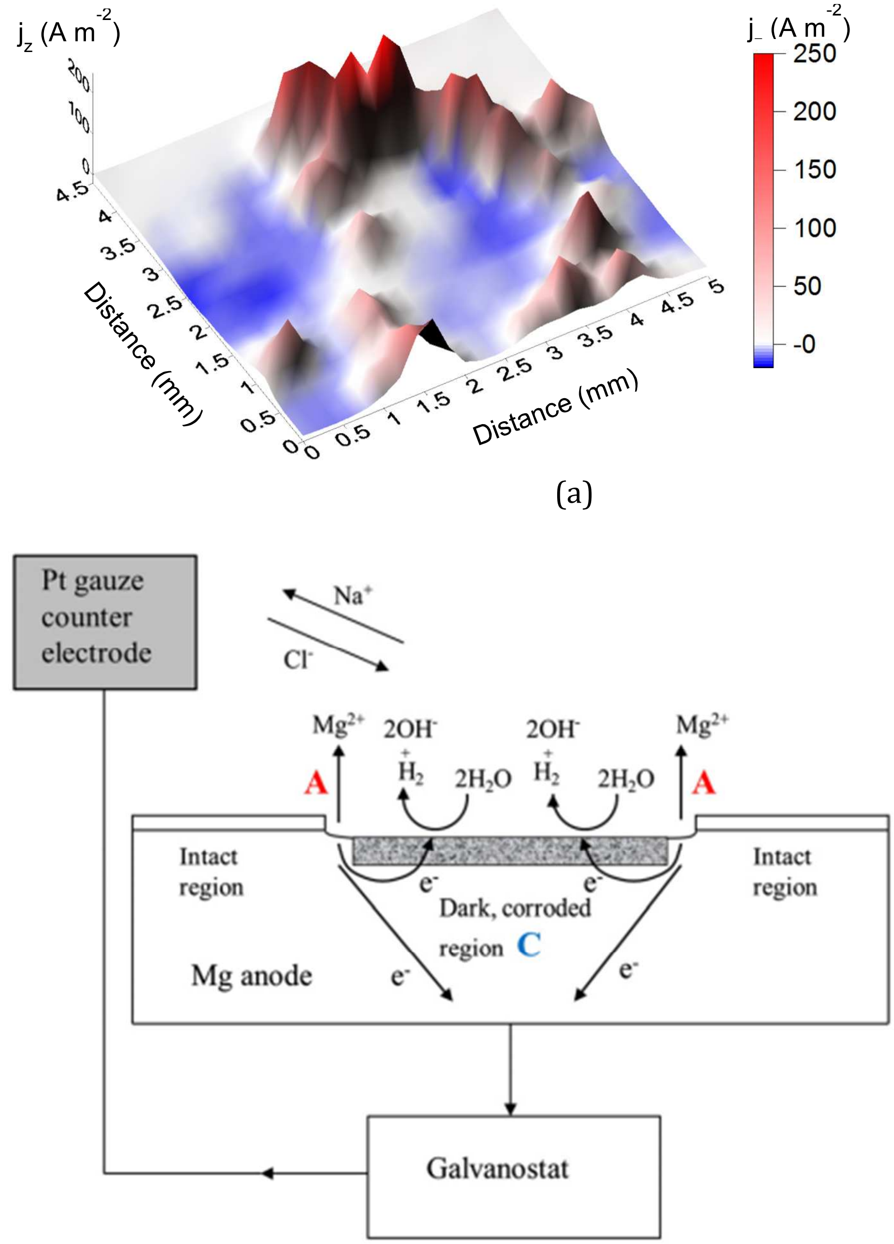

(a)

(b)

Figure 4. a) Current density map determined by SVET during polarization of pure Mg at a fixed anodic current density of 1 mA/cm^2.[16] b) Schematic showing the proposed model for anodic HE, whereby the dark, previously corroded area acts as a net cathode even during anodic polarization. Reprinted with permission from Elsevier.

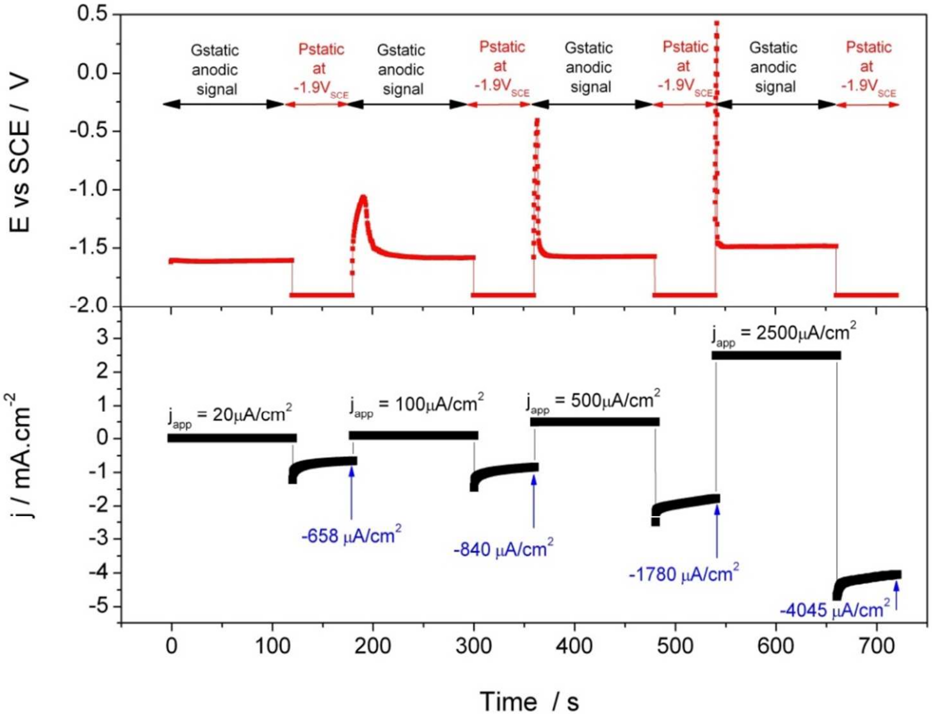

Figure 5. Results of cycled anodic galvanostatic polarization at different current densities and cathodic potentiostatic polarization at -1.9 V SCE showing the increase in cathodic current following anodic polarization at higher currents.[18] Reprinted with permission from Elsevier.

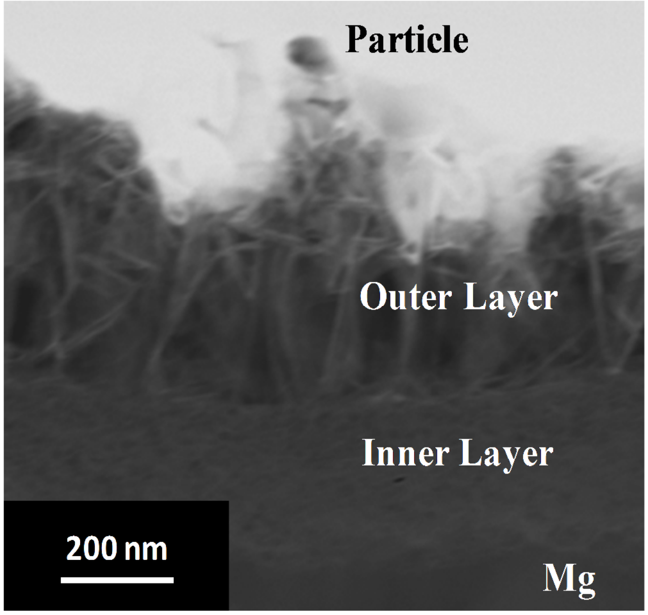

Figure 6. TEM image of the bilayered corrosion film formed on a pure Mg sample during anodic polarization showing an example of an Fe rich particle in the outer layer.[19] Reprinted with permission from Elsevier.

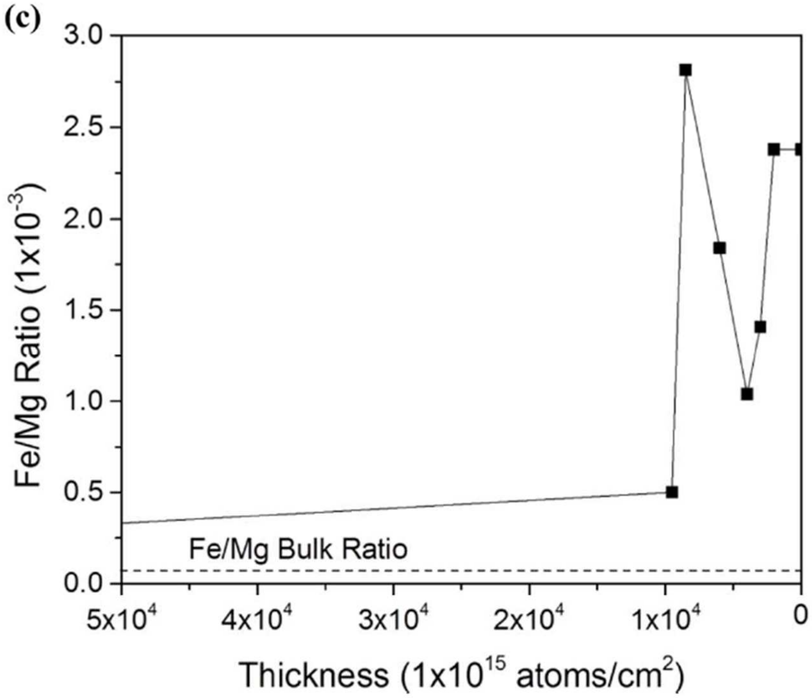

Figure 7. Fe/Mg ration as a function of depth from the surface as determined from RBS data for a sample polarized at -1.625 V SCE for 24 h showing Fe enrichment.[12]

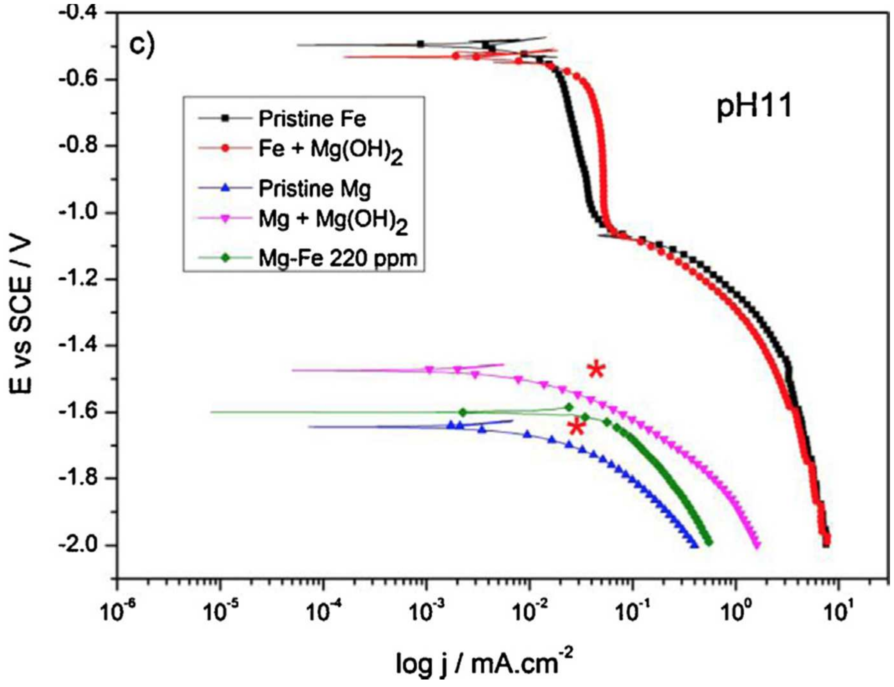

Figure 8. Cathodic polarization curves for pure Fe and Mg as well as these materials coated with $Mg(OH)_2$ in 0.1 NaCl solution.[22] Reprinted with permission from Elsevier.

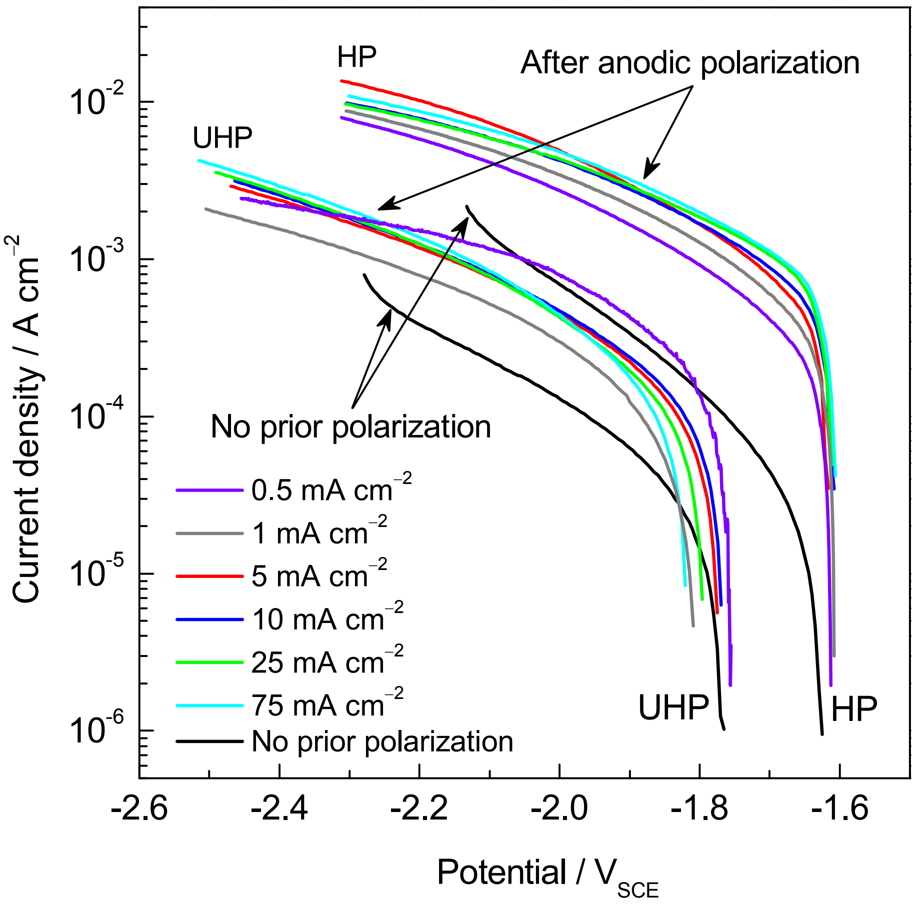

Figure 9. Cathodic polarization curves (non-IR-corrected) measured on HP and UHP Mg samples after galvanostatic anodic polarization.[5] Reprinted with permission from Elsevier.

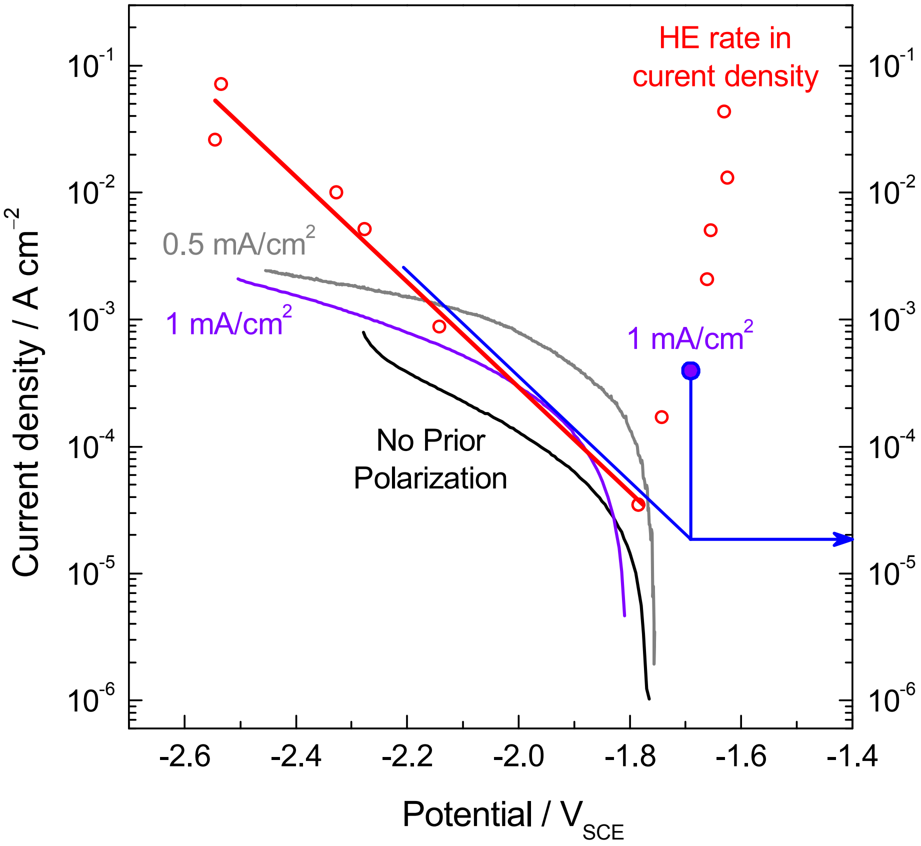

Figure 10. Cathodic polarization curves (non-IR-corrected) from selected UHP Mg samples in Figure 9 along with the current density calculated from the HE rate during galvanostatic polarization tests (open circles) plotted against measured and IR-corrected potential.[5] Also shown are lines describing the method for determination of the effect of the corrosion film and impurities on anodic HE. The arrow pointing to the right shows the value of HE rate from the film and impurities predicted by extrapolation for the case of 1 mA/cm^2.

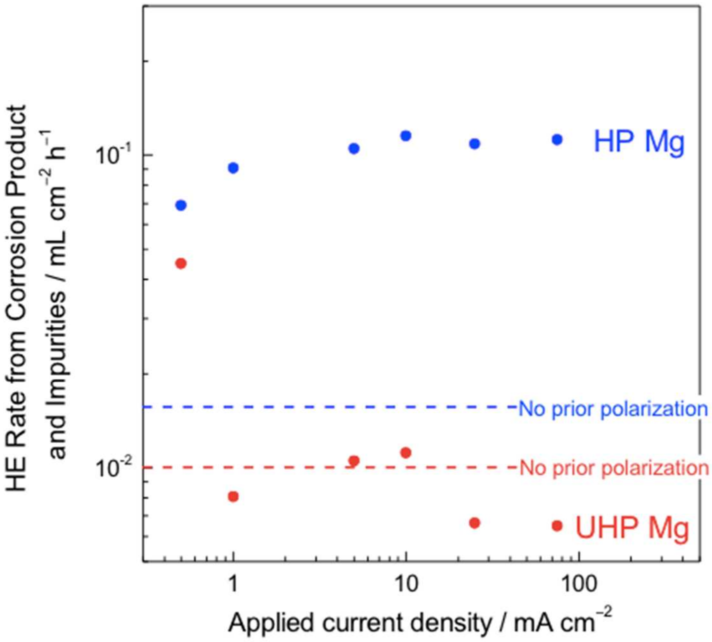

Figure 11. HE rate from the corrosion product and surface enriched impurities for HP and UHP Mg determined by extrapolation as shown in Figure 10.[5] Note that 1 x 10^{-2} ml/cm^{2}h = 2.2 x 10^{-5} A/cm^2. Reprinted with permission from Elsevier.

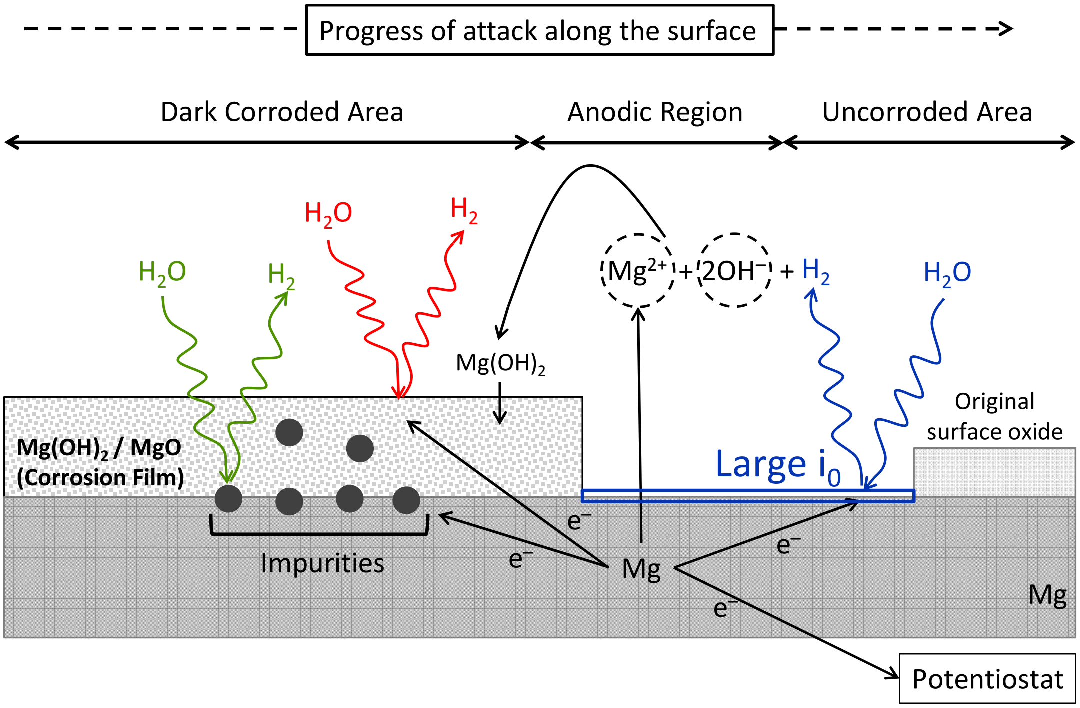

Figure 12. A schematic representation of the anodic HE process that distinguishes the contribution of corrosion film, accumulated impurities, and anodic area.

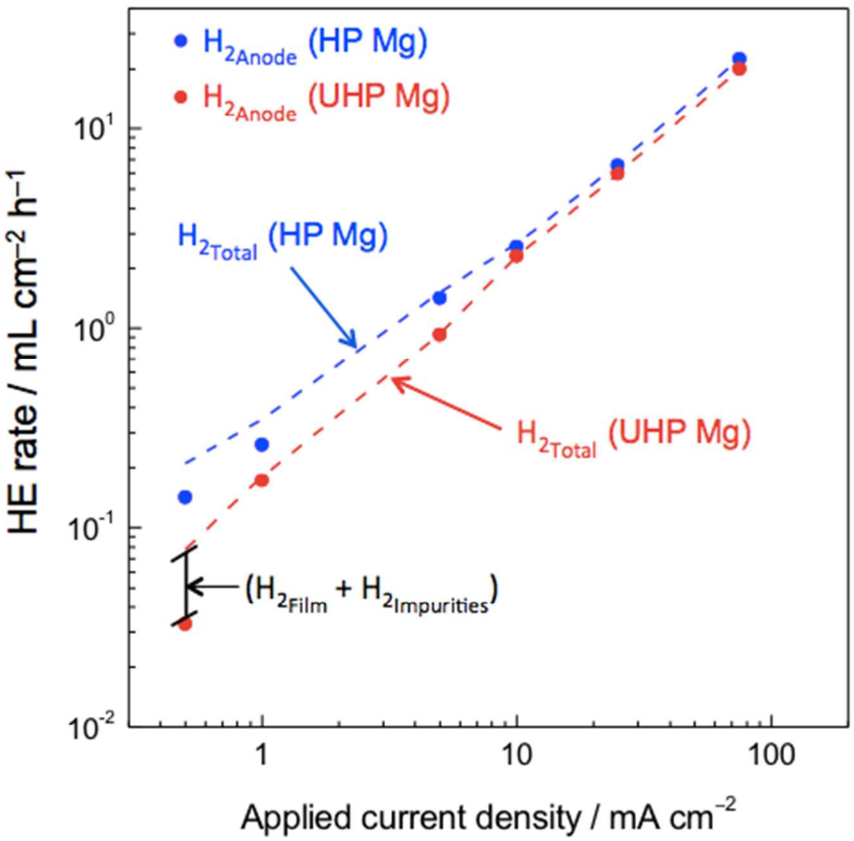

Figure 13. Anodic HE rate as a function of anodic applied current density.[5] The dashed lines are HE_{tot} measured volumetrically and the symbols are the HE rates from the dissolving anode sites, determined by subtracting the values of HE from the film and impurities shown in Figure 11. Reprinted with permission from Elsevier.

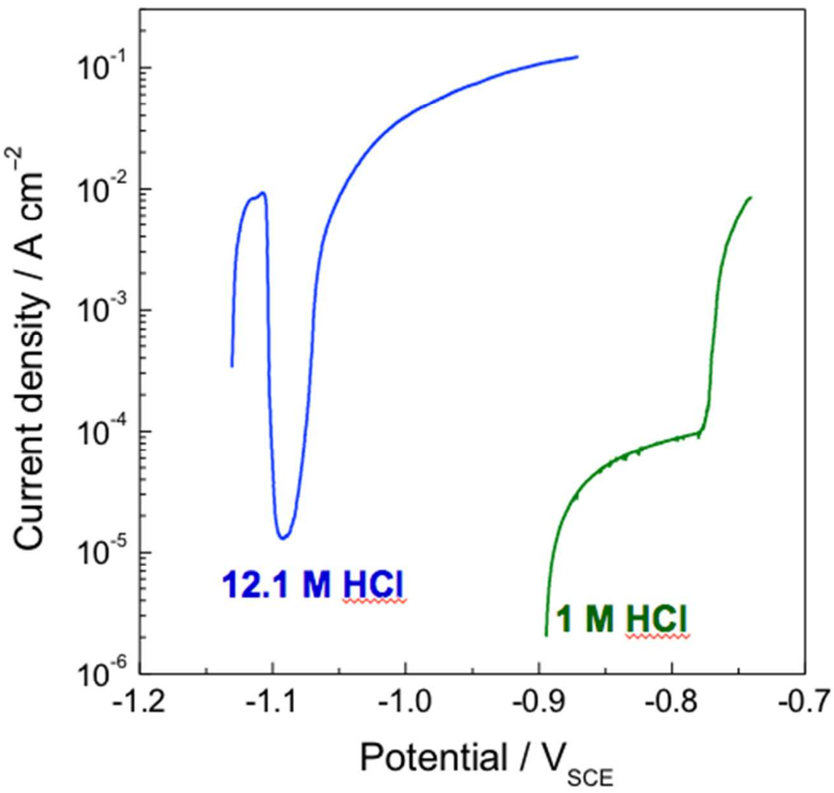

Figure 14. Potentiodynamic polarization curves for 99.99% Al in HCl solutions measured at 0.1 mV/s.

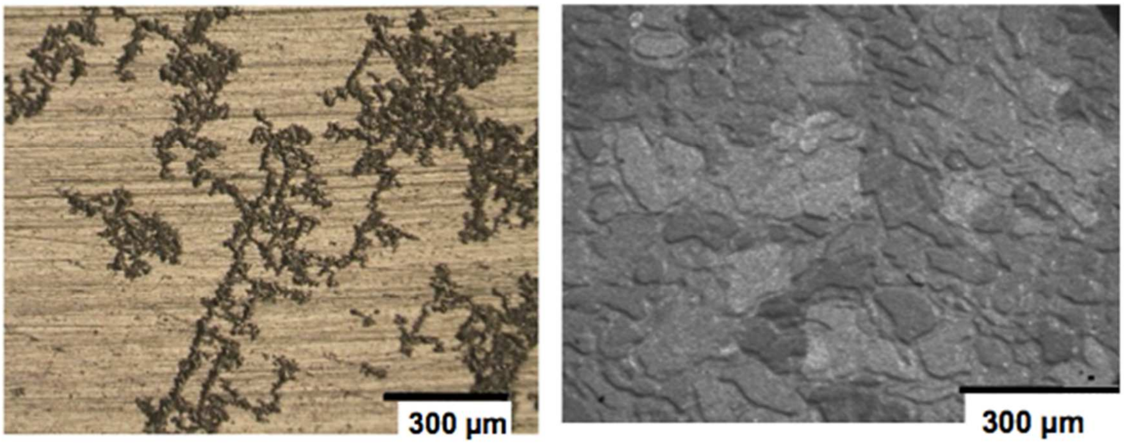

a) b)

Figure 15. Optical microscope images of the surfaces of pure Al following measurements of the polarization curves. a) 1 M HCl, b) 12.1 M HCl

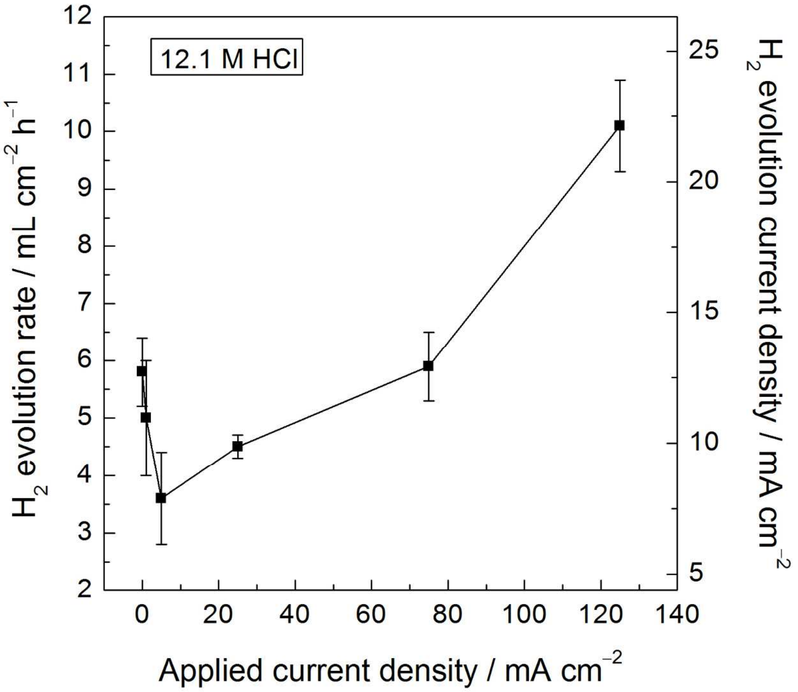

Figure 16. HE rate measured on pure Al in 12.1 M HCl solution at different applied anodic current densities. The polarization time was 300 s for each case.

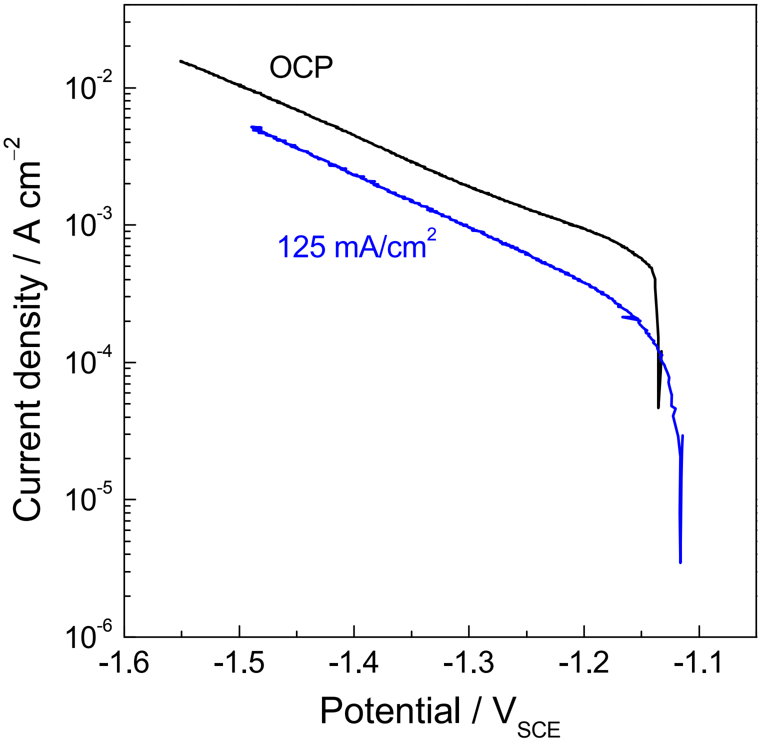

Figure 17. Cathodic polarization curves measured on a freshly prepared surface and on a sample that was previously polarized at 125 mA/cm^2 for 300 s.